MODELING OF A SOLAR DRIVEN LIQUID DESICCANT AIR-CONDITIONER EQUIPPED WITH DESICCANT STORAGE

Christopher McNevin[1] and Stephen J. Harrison[2]
[1,2]Department of Mechanical and Materials Engineering, Queen's University, Kingston, Canada

ABSTRACT

TRNSYS was used to develop a simulation of a solar liquid desiccant air-conditioner system. A stratified desiccant storage tank model was developed and integrated into the system model to determine the system's performance when using different tank and solar array sizes. The new tank model used the mass-fraction and temperature of the desiccant to determine its density and model the tank stratification. Increased desiccant storage allowed for a greater solar contribution to the thermal requirements of the system. Specifically, the storage allowed surplus energy to be gathered during times of peak solar availability and stored in the desiccant for later use. The model results, in the Toronto climate, indicated the system's solar fraction was increased by up to 64% through the use of desiccant storage. The use of a stratified desiccant tank also contributed to improved dehumidification as higher desiccant concentrations were delivered to the conditioner.

INTRODUCTION

HVAC systems have typically required large amounts of electrical power to provide high quality air conditions to the occupants of a building. During the summer season, the load is comprised of sensible and latent cooling (i.e., temperature reduction and dehumidification). Traditionally, systems have used vapor compression systems (VC) that excelled in meeting the sensible load, but were limited in their capacity to dehumidify the air. To reduce humidity, VC systems over-cooled the air to reach the dew point and condense the moisture out. The air would then be reheated to a comfortable temperature. This weakness is compounded since the sensible cooling load in many climates was found to be less than the latent load (Harriman, Plager, and Kosar, 1997), so a cooling technique that can target the latent load is desired.

LDAC Systems

A solar thermally driven liquid desiccant air-conditioner (LDAC) can provide latent cooling while drawing minimal electricity. LDAC units use a hygroscopic solution to remove moisture from the process air-stream. The water removed from the air-stream dilutes the desiccant-solution as it is absorbed. Consequently, the dilute desiccant-solution is pumped to a regenerator where heat is used to drive water from the solution into a scavenging air-stream.

This system can reduce the electrical demand, as humidly control is achieved chemically rather than mechanically. In addition, the unit investigated can be driven by relatively low temperature thermal energy (60°C to 95°C). Solar thermal energy, supplemented by a natural gas boiler, was used as the heat source in this study. Waste process heat could be used in other scenarios.

Several methodologies are used to condition air with liquid desiccants. Many are based on packed beds (Fumo and Goswami, 2002; Stevens, Braun, and Klein, 1989; Gandhidasan, 2004). In packed-beds, the process air is treated in the conditioner. Pre-cooled desiccant-solution is sprayed over a bed of random or structured packing materials. The desiccant comes into direct contact with the process air-stream being blown through the bed. The direct contact allows for the transfer of water into the desiccant. The reverse process occurs in the regenerator, where the preheated desiccant-solution comes into contact with a scavenging air-stream. The problem with packed-bed designs is the carry-over of desiccant droplets into the air-streams. The desiccant used can be highly corrosive and can cause damage to downstream equipment.

A different design using an internally cooled/heated, low-flow, laminar falling-film configuration was analyzed for this study (Lowenstein, Slayzak, and Kozubal, 2006). This system uses a thin falling-film of desiccant-solution on the outside of a series of temperature controlled parallel plates. The carry-over of desiccant into the airstream is effectively eliminated by the use of the low-flow laminar films. A wicking material on the surface of the plates helps to retain the desiccant-solution and ensure the full wetting of the plate.

A schematic of the LDAC system used for this study is shown in Fig. 1. A lithium chloride and water solution was used as the desiccant. This system is described in great detail in previous experimental studies on the unit used in the present study (Jones, 2008; Crofoot, McNevin, and Harrison, 2014).

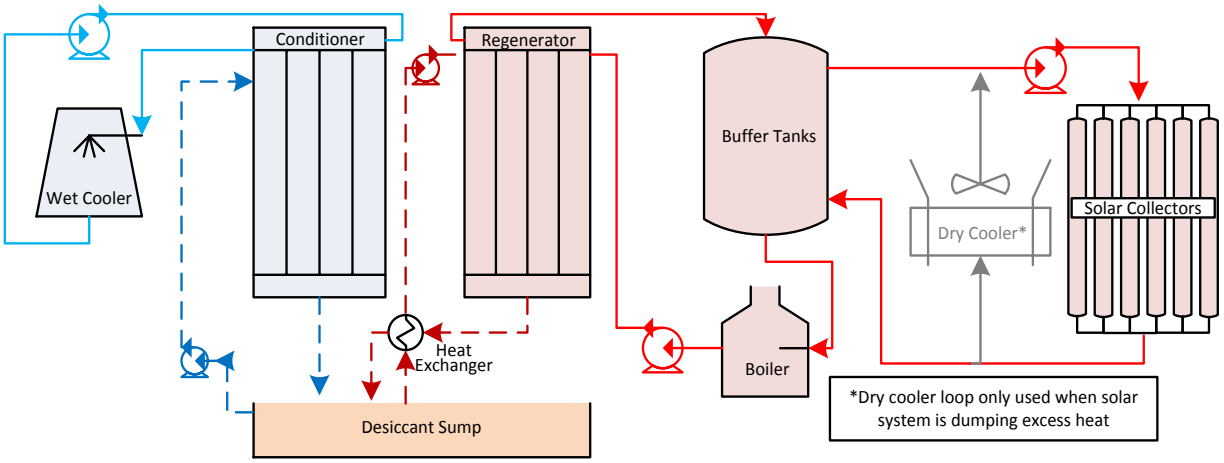

Fig. 1. Simplified system layout showing the LDAC unit and the associated heat generation and rejection sub-systems.

These studies showed the potential of the system but the results also indicated areas where improvements could be made. The electrical coefficient of performance (COP_e = $\dot{Q}_{total,cooling}$ / $\dot{Q}_{elec}$) found by Crofoot et. al (2014) ranged between 1.8 and 2.8, with an average of 2.4. The thermal coefficient of performance (COP_t = $\dot{Q}_{total,cooling}$ / $\dot{Q}_{heat,in}$) ranged between 0.26 and 0.53 with an average of 0.40. $\dot{Q}_{total,cooling}$ was the total cooling rate of the system, $\dot{Q}_{heat,in}$ was the total rate of thermal energy input and $\dot{Q}_{elec}$ was the electrical power consumption. These performance indices showed room for improvement. Increases in COP can be made by either increasing the total cooling rate or, decreasing the heat or electrical input required. McNevin and Harrison (2014) modeled the use of heat recovery techniques to improve these values.

Another key performance variable is the solar fraction (*SF*) (Eq. 1). The solar fraction is the ratio of the amount of energy required by the load ($\dot{Q}_l$) to the amount provided by the solar array ($\dot{Q}_u$). For the current work it was easier to determine the value using the boiler input rate ($\dot{Q}_b$). Crofoot et al. (2014) found this value to be 0.4. This value could not be greatly improved by increasing the solar thermal array's size as during times of peak solar availability, even with the currently sized 95 m^2 solar thermal array, some heat had to be vented by a fan coil unit to prevent the array from over-heating. To enumerate this concept, the solar utilization (*SU*) can be used (Eq. 2). *SU* is a measure of the amount of heat gathered by the solar array compared to the amount of heat rejected by an over-heat protection dry cooler unit ($\dot{Q}_{rej}$).

$$SF = \frac{\dot{Q}_u}{\dot{Q}_l} = 1 - \frac{\dot{Q}_b}{\dot{Q}_l} \quad (1)$$

$$SU = 1 - \frac{\dot{Q}_{rej}}{\dot{Q}_u} \quad (2)$$

Desiccant Storage

To take advantage of a larger solar thermal array, a desiccant storage tank and new control system have been modelled. It was hypothesized that this could be used to greatly increase the solar fraction of the system. The excess solar energy could be stored thermally in large water tanks, but this method suffers from the low energy storage density of water and high thermal losses. This excess energy could be stored chemically in the desiccant itself, in a lossless, high energy density form (Kessling, Laevemann, and Kapfhammer, 1998).

Testing various array sizes, control systems, and storage volumes experimentally would be a prohibitively expensive and time consuming endeavour. Instead, to study the feasibility of a desiccant storage system for the low-flow LDAC system, a system scale simulation can be used. The present work updated the TRNSYS model initially developed by Andrusiak et al. (2010), updated by McNevin and Harrison (2014).

The previous work used a well-mixed desiccant sump model. The present work builds on this model of a well-mixed sump to create a new TRNSYS TYPE that accounts for the density stratification expected from a large desiccant storage tank combined with the low desiccant-solution flow rates of the LDAC system.

SIMULATION

LDAC Model

Several methods exist for modeling the operation of a LDAC system. The most common are either detailed numerical models (Factor & Grossman, 1980; Fumo & Goswami, 2002) or effectiveness models (Gandhidasan, 2004; Stevens et al., 1989). For the current study, an effectiveness model, based on the work by Andrusiak et. al (2010) and updated and verified by Crofoot (2012) and McNevin and Harrison (2014), was used. The model was developed using TRNSYS, a software platform that allows the operation of entire systems to be simulated under realistic conditions (TRNSYS, 2006). The TRNSYS simulation studio is used to model different components using either built-in TYPEs or user created TYPEs coded in FORTRAN. It also allows for flexibility through the easy modification, addition, or removal of these components. This makes it a suitable program for system design and improvement as many different variations can be tested.

The regenerator and conditioner were modeled using previously developed custom TYPEs (Andrusiak et al., 2010). For each component, three effectiveness values were used to find the outlet conditions of the air, water, and desiccant-solution streams.

The first effectiveness value, ε_w, (Eq. 3) determined the amount of mass transferred between the air and desiccant stream. The mass transferred was governed by the humidity ratios (ω_{in} and ω_{out}), which in turn were governed by the partial pressures of water vapour in the air ($p_{wa,in}$ and $p_{wa,out}$). The minimum partial pressure value, $p_{wd,min}$, used in the conditioner, was assumed to be the water vapour partial pressure of air in equilibrium with the desiccant-solution at the cooling water inlet temperature and at the inlet concentration of the desiccant-solution.

The enthalpy effectiveness, ε_h (Eq. 4) was used to determine the outlet-air enthalpy, $h_{a,out}$, and from that, the outlet-air temperature was calculated using standard psychrometrics. The values for the conditioner minimum-enthalpy, $h_{a,min}$, and regenerator maximum-enthalpy, $h_{a,max}$, were assumed to be the enthalpy of air at the same conditions as used for the mass transfer effectiveness.

The third effectiveness, ε_d, (Eq. 5) was used to find the outlet desiccant temperature, $T_{d,out}$, using the cooling water, $T_{cw,in}$, and heating water, $T_{hw,in}$, inlet temperatures as the minimum conditioner value and maximum regenerator value. $T_{d,in}$ was the inlet desiccant temperature.

$$\varepsilon_w = \frac{\omega_{in} - \omega_{out}}{\omega_{in} - \omega_{\min/\max}} = \frac{p_{a,in} - p_{a,out}}{p_{a,in} - p_{d,\min/\max}} \tag{3}$$

$$\varepsilon_h = \frac{h_{a,in} - h_{a,out}}{h_{a,in} - h_{a,\min/\max}} \tag{4}$$

$$\varepsilon_d = \frac{T_{d,in} - T_{d,out}}{T_{d,in} - T_{cw,in/hw,\text{in}}} \tag{5}$$

System Model

Several built-in TRNSYS TYPEs were used in the simulation to model important system components. Further information on these TYPEs and the parameters used can be found in the TRNSYS documentation (Klein, 2006) and in previous work on the unit's simulation (Crofoot, 2012). Weather conditions were provided by a typical meteorological year data file for Toronto, Ontario. A list of built-in components used is provided in Table 1.

The system was simulated to run the conditioner on a daily schedule from 8 AM to 6 PM. All desiccant property values were calculated using correlations by Conde (2004).

Table 1. TRNSYS built-in TYPES used in the system model.

Type Number	Description
Type 2	differential controller
Type 3	pump
Type 6	natural gas boiler
Type 51	evaporative cooling tower
Type 60	hot water storage tank
Type 71	evacuated tube collectors
Type 91	heat exchanger
Type 511	dry cooler
Type 709	piping

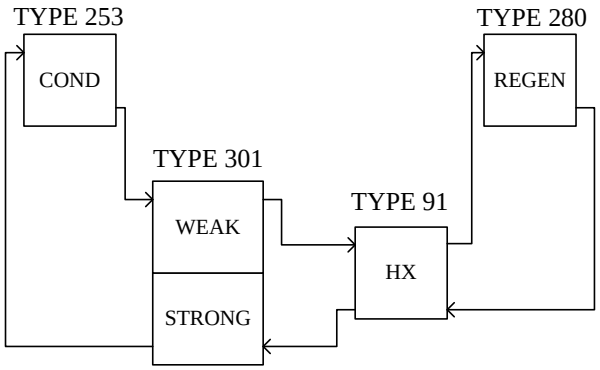

Fig. 2. A simplified schematic of the desiccant storage tank showing the weak and strong layer, and its connections to the LDAC components.

Desiccant Storage Model

The main focus of the present work was to create a new desiccant storage model and determine its effect on the LDAC system's performance. The sump model used in previous work was updated to create a variable volume, density stratified, two layer storage tank which was connected to the system as shown in Fig. 2.

Quinnell and Davidson (2012) studied a density stratified storage tank with different concentrations of salts for use in a heat pump application. The temperature differences in the two layers that formed caused internal natural convection currents that led to the formation of well mixed layers. This application also made use of a third layer of pure water that would not be present in a LDAC application.

Solar ponds are another classic example of this type of density stratification. Solar ponds, once fully operational, usually have top and bottom layers where internal convection currents create well-mixed layers separated by a thin non-convecting separation layer (Angeli & Leonardi, 2004). Work by Chepurniy and Savage (1974) showed that for a pond seeded with two layers, the time for a gradient to form can be as high as 652 days, and before this time, stratified layers existed.

For the LDAC unit, the concentration differences between the weak (i.e., diluted solution from the conditioner) and strong (i.e., concentrated solution from the regenerator) will form the stratified layers. The temperature differences of the desiccant leaving the conditioner (cold) and the regenerator (hot) will generate the driving forces for the internal convection currents that mix each layer, without mixing the weak and strong layers.

It is assumed that due to the low flow rate design of the LDAC unit, a minimum amount of mixing would occur. In a physical tank, a manifold on the inlets and outlet should be used to reduce the mixing effects of the fluid mass flows. The tank would also require an air space at the top as well as a vent to allow for the expected changes in volume as the desiccant absorbs or rejects moisture.

TYPE 301 was created to model the desiccant storage tank. The inputs, parameters and outputs are fully listed in Table 2.

Each layer required the solution of three differential equations to determine the conditions of the tank. A mass balance for each species, LiCl and water, as well as an energy balance enabled the calculation of the storage tank's outlets. The balances were simplified to enable the system to be solved by TRNSYS. The density, ρ^{i-1}, and mass, m^{i-1}, of the material in the each layer were assumed to be at the values of the previous time step (i.e., *i-1*). The mass balance used for the desiccant species is shown in Eq. 6.

Table 2. TYPE 301 parameters and input variables.

No	Parameters	Inputs
1	The initial volume of the strong layer	Inlet mass flow rate of the desiccant-solution into the strong layer
2	The initial mass fraction of the strong layer	Inlet temperature of the desiccant-solution flowing into the strong layer
3	The initial temperature of the strong layer	Inlet mass fraction of the desiccant-solution flowing into the strong layer
4	The initial volume of the weak layer	Volumetric flow rate of the desiccant-solution leaving the strong layer
5	The initial mass fraction of the weak layer	Inlet mass flow rate of the desiccant-solution into the weak layer
6	The initial temperature of the weak layer	Inlet temperature of the desiccant-solution flowing into the weak layer
7	The heat capacity of the desiccant-solution	Inlet mass fraction of the desiccant-solution flowing into the weak layer
8	The overall heat transfer coefficient at the interface between the strong and weak layers	Volumetric flow rate of the desiccant-solution leaving weak layer
9	The heat transfer coefficient for the heat losses to the surroundings	Ambient temperature
10	Perimeter of the tank	
11	Cross sectional area of the tank	

$$\frac{dm^i_{LiCl}}{dt} = \dot{m}^i_{in} X^i_{in} - \dot{V}^i_{out} \rho^{i-1} \frac{m^i_{LiCl,}}{m^{i-1}} + \frac{\rho^{i-1} D^{i-1} A_c}{\Delta z} \left(X^{i-1}_{other} - \frac{m^i_{LiCl}}{m^{i-1}} \right) \quad (6)$$

The change in mass of LiCl at the current time step, m^i_{LiCl}, was equal to the total mass going into the layer at the current time step, $\dot{m}^i_{in}$, multiplied by the inlet mass fraction, X^i_{in}, minus the mass of desiccant leaving the layer. The mass leaving the layer was calculated from the total volumetric outflow of the layer, V^i_{out}, multiplied by the layer's density and mass fraction. The mass fraction was determined by the mass of LiCl at the current time step, m^i_{LiCl}, divided by the total mass of the desiccant-solution in the layer at the previous time step. The diffusivity term, D^{i-1}, accounted for the diffusion of LiCl from the strong layer into the weak layer. The diffusivity coefficient was determined using correlations from Conde (2004) using the conditions of the previous time step. The diffusion coefficient for each layer was found and then averaged to maintain the mass balance. A_c was the cross sectional area of the tank. $X^{i-1}{}_{other}$ was the mass fraction of the adjacent layer at the previous time step. Δz was the height of the layer.

A second mass balance (Eq. 7) was needed to model the water in the storage tank. This equation was modified from that used for LiCl by removing the salt diffusion term and by calculating the mass fraction of water rather than that of the desiccant ($1\text{-}X^i_{in}$).

$$\frac{dm^i_w}{dt} = \dot{m}^i_{in} \left(1 - X^i_{in}\right) - \dot{V}^i_{out} \rho^{i-1} \left(\frac{m^i_w}{m^{i-1}} \right) \quad (7)$$

balance (Eq. 8) required several assumptions. The heat capacity, c_p, was assumed constant. The heat transfer coefficients between the tank and its surroundings, U_{tank}, and the interface between layers, U_{int}, were also assumed constant. The transfer of energy associated with the heat of dilution and the diffusion mass transfer was small enough to be considered negligible.

$$\frac{d(c_p\, m^{i-1} T^i)}{dt} = (c_p \dot{m}^i_{in} T^i_{in} - c_p \dot{V}^i_{out} \rho^{i-1} T^i) - U_{tank} A_s (T^i - T^i_{amb}) - \ldots$$
$$\ldots U_{int} A_c (T^i - T^{i-1}_{other}) \quad (8)$$

The energy transfer between the layers was calculated using the difference between the temperature of the layer in question, T^i, and the temperature of the adjacent layer at the previous time step, $T^{i-1}{}_{other}$, along with the cross sectional area and U_{int}. The heat lost to the surroundings was found using the difference between T^i, and T^i_{amb}, multiplied by U_{tank}, and the surface area of the layer exposed to the surroundings, A_s. Losses from the top and bottom of the tank were assumed negligible. The energy change due to the inlet and outlet streams was calculated from the outlet stream's energy being subtracted from the energy of the inlet stream, where T^i_{in} was the temperature of the inlet desiccant-solution stream.

The differential equations were solved using Eq. 9. This is an analytical solution to differential equations of the form $dY/dt = aY + b$. The differential equations (Eq. 6, 7, and 8) were rearranged to find the coefficients a and b.

$$Y^i = \left(Y^{i-1} + \frac{b}{a} \right) e^{a\Delta t} - \frac{b}{a} \quad (9)$$

The storage tank model was designed to be flexible and as such, several possible scenarios were accounted for in the coding. The LDAC unit used dissimilar desiccant-solution pump flow rates and run times in the regenerator and conditioner. Therefore, the possibility existed for one of the layers to be emptied (this would most likely be the bottom strong layer as the conditioner used a higher solution flow rate). In the event of a layer emptying, the model was programmed to begin drawing from the other layer. Once the opposing layer was re-established, the model would revert to drawing from that layer (Fig. 3).

A small dead band was included to reduce the hysteresis effects. This dead band allowed the emptied layer to refill slightly before the draw switched source layers.

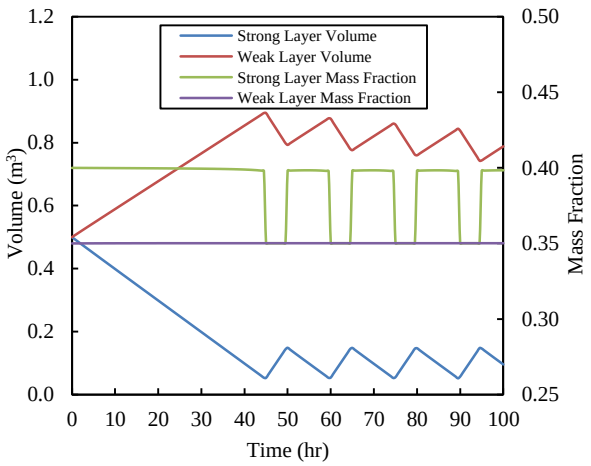

Fig. 3. TYPE 301 operation when forced to empty the strong layer. Layer is shown to be re-established before being emptied again repeatedly.

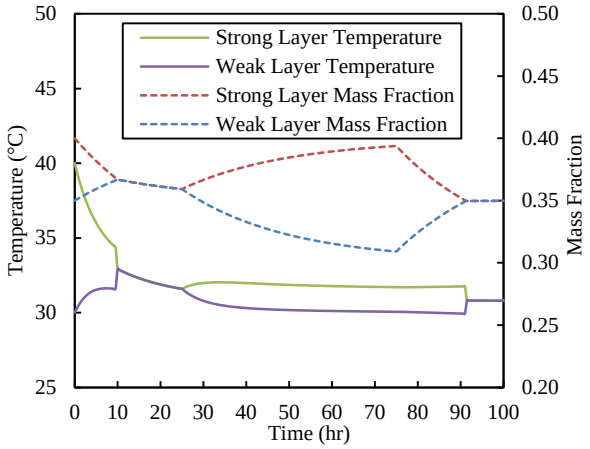

Fig. 4. TYPE 301 operation when forced to mix, re-stratify and then mix again.

Another possible event was the mixing of the tank. This would occur if the density of the layers equalized due to concentration or temperature changes. The model was programmed to mix the two layers if the densities equalized by resizing each layer into half the total volume of the tank and giving each layer identical conditions for temperature and concentration as determined by energy and mass balances. This allowed for re-establishment of stratification as conditions changed (Fig. 4).

This model had several weaknesses. The use of several values from the previous time step in the differential equations required the use of small time steps to minimize the difference between each time step which increased the computational time. Also, the internal natural convection currents were not modeled but these may affect both heat and mass transfer across this boundary. The thin non-convecting mixed layer seen experimentally by Quinnell and Davidson (2012) could act as an insulating layer that would negate the effects of these currents.

Another assumption of the model was that the inlet and outlet fluid velocity and momentum would not disrupt the stratification of the tank. As long as the system uses relatively low flow rates, and with the use of proper manifolds, the chances the layers mixing in a physical system are low. The problem of mixing when one layer is emptied is another issue with this model. If one layer nears an empty state, the simulation instantly switches the outlet conditions to the conditions of the other layer. In reality there would likely be some mixing at this point. Allowing the layer to partially fill before resuming output should help simulate this mixing effect, but it does not fully solve the problem. The model also assumes the entire tank would mix instantly if stratification was lost. Modelling additional layers would reduce this problem, but in normal operation loss of stratification was very rarely seen so it is not a major concern for this application.

RESULTS AND DISCUSSION

The purpose of desiccant storage was to increase the solar fraction of the system. The larger desiccant tank was hypothesized to allow for larger volumes of desiccant-solution to be strengthened during times of peak solar availability. The stored strong desiccant-solution could be utilized during times of low solar availability rather than running the natural gas boiler. The availability of higher concentration desiccant-solution for the conditioner was also expected to increase the cooling rates. A higher COP_t was expected since the regenerator would be rejecting moisture from lower mass fraction desiccant-solution. The weaker solution would have a higher vapour partial pressure and would thus increase the driving force for mass transfer without increasing the thermal requirements of the system.

Three different regenerator control methods were simulated to determine the best method utilizing the stored desiccant. The first method used the original (Andrusiak, Harrison, and Mesquita, 2010) simulation's controller that activated the regenerator when the process air-stream's relative humidity was above 30%. This method did not take advantage of the increased amount of desiccant available and thus significant performance gains were not seen in simulation results.

Control method two ran the regenerator using only solar power (when solar power was available), except when the process-air's relative humidity was above 30% in which case the boiler was activated to ensure a minimum heating water temperature of 80°C.

Control method three used the same idea as the second method, but activated the boiler when the mass fraction of the desiccant-solution entering the conditioner (i.e., the strong layer mass fraction) was below 37%. The boiler would then run until the solution's mass fraction was increased to 40%.

These two methods both reliably ran the system during June-August cooling season. Method two could provide slightly higher air cooling rates, but the COP and solar fraction values were reduced. Method three provided the best all round performance and will be analyzed in greater detail.

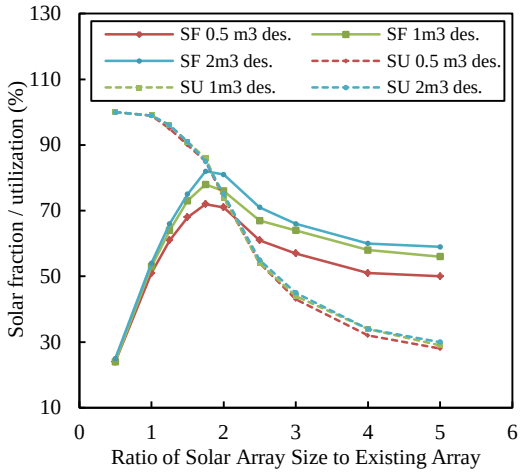

Fig. 5. Solar fraction and solar utilization ratios of systems simulated using different sized solar arrays and tanks.

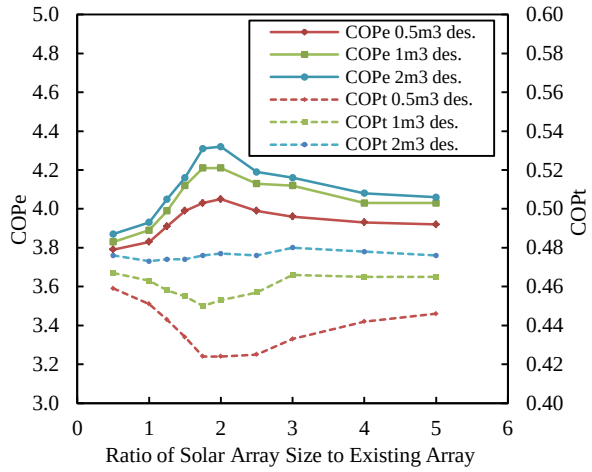

Fig. 6. COPs of systems simulated using different sized solar arrays and desiccant storage tanks.

Different sizes of solar thermal arrays were simulated with various sizes of desiccant storage. The hot water storage volume and the total water flow rate through the collectors were maintained at the same ratio to collector area as in the initial simulation. For example, in a simulation run with a solar array twice as big as the original, the collector water flow rate was doubled and the hot water buffer tank volume was also doubled.

The *SF* and *SU* for the simulations run using control method three were analysed (Fig. 5) as well as the COPs (Fig. 6). Each data point on the plots represents the average value achieved over the course of a June to August cooling season run using Toronto weather data. The three different sizes of 0.5 m^3, 1.0 m^3 and 2.0 m^3 of desiccant storage were tested. The strong layer was initially at 40% mass fraction and the weak layer was at 38% mass fraction. The solar array system was sized at ten different multiples of the existing state from half sized to five times larger than the existing design.

The results indicated an obvious point of maximum performance. A solar multiplier of 1.75 was found to provide the greatest *SF* while maintaining a reasonably high *SU*. This was found to be true for all sizes of desiccant storage simulated. The COP_e was also is at a maximum point in this configuration. The COP_t responded in the opposite fashion to the COP_e. Due to this the COP_t was at a minimum value at this point. While this was not a desirable outcome, the need for extra heat was offset due to the increase in solar energy used by the system which still led to a higher *SF*. The total and latent cooling rates were also at a high point at this size, although the variation with array size is not as extreme as with the other performance metrics.

When using smaller arrays, the boiler was required more often to heat the water as the solar array could not supply enough heat. The array was incapable of providing enough heat to the regenerator so the array never overheated, even during peak solar times. Consequently, the *SU* was higher as the dry cooler was rarely activated. The lack of sufficient solar energy meant that the heating water temperature never increased over 80°C, reducing the amount of moisture rejected by the regenerator leading to lower concentration desiccant and hence, reduced latent cooling rates.

With a solar size ratio of 1.75, more heat was supplied to the regenerator by the array. This reduced the need for the boiler to provide energy. In addition to this, the solar array did not reject heat until the water reached 95°C, meaning that hotter water was supplied to the regenerator during peak solar times, compared to smaller array sizes where the water was maintained at 80°C by the boiler. This increased the moisture rejection rate and raised the concentration of the solution and thus, improved the latent cooling rate.

The array overheated for longer periods of time as the array multiplier value increased over 1.75. This caused the heat dump mechanism to be activated for longer periods of time. As a result, the solar utilization and fraction were reduced since the energy collected by the array was wasted. When the heat dump was activated, the LDAC system switched over to run using the boiler as the principle heat source. This reduced the water temperatures back down to 80°C as seen with smaller array sizes, leading to similar results in thermal and electrical COP.

Table 3. Performance of TYPE 301 using 2.0 m^3 sump volumes and a solar multiplier of 1.75 compared to the same system simulation using the original desiccant sump (TYPE 299). Simulations run using Toronto weather data from July to August inclusive.

Simulation	COP_t			COP_e			SF			Q_{total}			Q_{latent}		
	avg	max	min	avg	max	min	avg	max	min	avg	max	min	avg	max	min
	~	~	~	~	~	~	%	%	%	kW	kW	kW	kW	kW	kW
TYPE 299	0.44	0.67	0.27	3.67	5.04	1.79	50	71	-8.0	12.2	16.9	7.80	13.2	17.7	8.81
TYPE 301	0.48	6.36	0.28	4.31	7.42	2.79	82	100	2.0	12.9	20.6	7.76	14.1	22.3	8.44

The performance was better, as expected for larger volumes of stored desiccant, with higher values of COP_t, COP_e, and solar fraction as the storage volume increased. The solar utilization also showed higher values with larger storage volumes, but the differences were much smaller.

A comparison can be made to highlight the improved performance provided by the largest desiccant storage system modeled over a simulation using the same input weather data and time frame and the original desiccant sump, labeled TYPE 299 (Table 3).

The system did not take full advantage of the desiccant storage as evidenced by the findings that the optimal array multiplier value was the same for all tank sizes. Performance improvements seen with larger tank sizes were attributed to the larger mass of LiCl increasing the average mass fraction of the desiccant under similar cooling loads. This indicated that the regenerator itself was the limiting factor. Maximising the performance of larger solar array systems and the additional thermal energy they provide would require the regenerator to be able reject more moisture over a shorter period of time. This could be accomplished by adding a second regenerator, or increasing the size of the current regenerator and increasing the desiccant and hot water flow rates.

CONCLUSIONS

Large scale desiccant storage for a solar thermally driven LDAC system was modeled using a new custom component in TRNSYS. To take advantage of the load shifting made possible by the storage volume, larger solar array areas were simulated to find the optimum point.

Using an array multiplier of 1.75 (i.e., 1.75 times larger than the installed 95 m^2 area array) the 2 m^3 desiccant storage system and new control method provided a solar fraction 64% higher than the original system. The air cooling rates and the COPs were also improved to a lesser extent by the use of this system.

The limitation of the system for additional performance was found to be the regenerator, as a limit was reached with the amount of moisture that could be rejected during the operation period.

ACKNOWLEDGEMENTS

The authors would like to thank Natural Resources Canada (NRCan), the Smart Net-Zero Energy Buildings Strategic Research Network (SNEBRN), and Natural Sciences and Engineering Research Council of Canada (NSERC) for their contributions to the research.

REFERENCES

Andrusiak, M., Harrison, S., & Mesquita, L. (2010). Modeling of a solar thermally-driven liquid-desiccant air-conditioning system. In *Proceedings of the 39th ASES National Conference* (pp. 1722–1729). Phoenix, Arizona.

Angeli, C., & Leonardi, E. (2004). A one-dimensional numerical study of the salt diffusion in a salinity-gradient solar pond. *International Journal of Heat and Mass Transfer*, *47*(1), 1–10. http://doi.org/10.1016/S0017-9310(03)00410-1

Chepurniy, N., & Savage, S. B. (1974). Effect of diffusion on concentration profiles in a solar pond. *Solar Energy*, *17*, 203–205.

Conde, M. (2004). Properties of aqueous solutions of lithium and calcium chlorides: Formulations for use in air conditioning equipment design. *International Journal of Thermal Sciences*, *43*(4), 367–382. http://doi.org/10.1016/j.ijthermalsci.2003.09.003

Crofoot, L. (2012). *Experimental Evaluation and Modeling of a Solar Liquid Desiccant Air Conditioner*. Queen's University.

Crofoot, L., McNevin, C., & Harrison, S. (2014). Performance evaluation of a liquid-desiccant solar air-conditioning system. In *EuroSun International Conference of Solar Energy and Buildings*. Aix-Les-Bains, France.

Factor, H., & Grossman, G. (1980). A packed bed dehumidifier/regenerator for solar air conditioning with liquid desiccants. *Solar Energy*, *24*(6), 541–550. http://doi.org/10.1016/0038-092X(80)90353-9

Fumo, N., & Goswami, D. (2002). Study of an aqueous lithium chloride desiccant system: Air dehumidification and desiccant regeneration. *Solar Energy*, *72*(4), 351–361. http://doi.org/10.1016/S0038-092X(02)00013-0

Gandhidasan, P. (2004). A simplified model for air dehumidification with liquid desiccant. *Solar Energy*, *76*(4), 409–416. http://doi.org/10.1016/j.solener.2003.10.001

Harriman, L. G., Plager, D., & Kosar, D. (1997). Dehumidification and cooling loads from ventilation air. *ASHRAE Journal*, *39*(11), 37–45.

Jones, B. (2008). *Field evaluation and analysis of a liquid desiccant air handling system*. Masters Thesis, Queen's University.

Kessling, W., Laevemann, E., & Kapfhammer, C. (1998). Energy storage for desiccant cooling systems component development. *Solar Energy*, *64*(4-6), 209–221. http://doi.org/10.1016/S0038-092X(98)00081-4

Klein, S. A. (2006). TRNSYS: A transient simulation program Ver. 16. Solar Energy Laboratory, University of Wisconsin-Madison. Madison, WI: Solar Energy Laboratory University Of Wisconsin-Madison. Retrieved from www.trnsys.com

Lowenstein, A., Slayzak, S., & Kozubal, E. (2006). A zero carryover liquid-desiccant air conditioner for solar applications. *ASME/Solar06, Denver, USA*, 1–11. http://doi.org/10.1115/ISEC2006-99079

McNevin, C., & Harrison, S. (2014). Performance improvements on a solar thermally driven liquid desiccant air-conditioner. In *Proceedings of The Canadian Society for Mechanical Engineering International Congress*. Toronto, Ontario.

Quinnell, J., & Davidson, J. (2012). Mass transfer during sensible charging of a hybrid absorption/sensible storage tank. *Energy Procedia*, *30*, 353–361. http://doi.org/10.1016/j.egypro.2012.11.042

Stevens, D., Braun, J., & Klein, S. (1989). An effectiveness model of liquid-desiccant system heat/mass exchangers. *Solar Energy*, *42*(6), 449–455. http://doi.org/10.1016/0038-092X(89)90045-5